KYBERNETIKA — VOLUME *56* (2020), NUMBER 4, PAGES 617–645

EXISTENCE AND SIMULATION OF GIBBS–DELAUNAY–LAGUERRE TESSELLATIONS

Daniel Jahn, Filip Seitl

Three-dimensional Laguerre tessellation models became quite popular in many areas of physics and biology. They are generated by locally finite configurations of marked points. Randomness is included by assuming that the set of generators is formed by a marked point process. The present paper focuses on 3D marked Gibbs point processes of generators which enable us to specify the desired geometry of the Laguerre tessellation. In order to prove the existence of a stationary Gibbs measure using a general approach of Dereudre, Drouilhet and Georgii [3], the geometry of Laguerre tessellations and their duals Laguerre Delaunay tetrahedrizations is examined in detail. Since it is difficult to treat the models analytically, their simulations are carried out by Markov chain Monte Carlo techniques.

Keywords: Laguerre–Delauay tetrahedrization, stationary Gibbs measure, Gibbs–Laguerre tessellation, MCMC simulation

Classification: 60K35, 60G55

1. INTRODUCTION

In the present paper, we study tessellations [9] as systems of space-filling cells in 3D. The cells are generated by locally finite point sets using an appropriate distance function. By allowing the generators to posses positive marks, the Voronoi tessellation is generalized to Laguerre tessellation [7]. This enables us to obtain more variable cells in terms of shapes and sizes. The drawback is that a generator does not have to be contained in the cell generated by it, or even may not generate a cell at all. The tessellation is described for theoretical purposes by the so-called hypergraph structure, cf. [3]. Randomness is entered in the tessellation models by considering random point processes as generators.

Gibbs point processes [1, 10] allow us to incorporate interactions between points in various ways. When extending the Gibbs point process from the finite volume to the infinite volume, cf. [2], its existence and uniqueness should be examined. The tool for proving the existence of a stationary Gibbs measure described in [3] covers many models, among them the Gibbs Voronoi and Gibbs Delaunay tessellations in two dimensions (2D), investigated in [4]. We continue this approach getting a proof of the existence of 3D Gibbs–Laguerre–Delaunay tessellations, i. e., two classes of dual models. In order to prove the existence of a stationary Gibbs measure, one does not need to consider

DOI: 10.14736/kyb-2020-4-0617

all possible point configurations, but may restrict only on those capturing some type of the pseudo-periodical behaviour. The Laguerre geometry of such configurations is of the interest and its knowledge will be the key part of the existence proofs. Two models based on the properties of Laguerre Delaunay tetrahedra and two on Laguerre cells will be considered.

In [13] an algorithm for the simulation of stationary Gibbs Laguerre tessellations in $\mathbb{R}^3$ was developed, inspired by 2D Voronoi case from [4]. One has to approximate the random tessellation in a bounded window and make use of finite volume Gibbs models. The Markov chain Monte Carlo methods [8] play a key role. In the present paper an extension to the simulation of 3D Gibbs Laguerre case is considered.

The paper is organized as follows: Section 2 presents the basic concepts necessary to understand Delaunay–Laguerre tessellation models. This section is purely deterministic. Randomness is introduced in Section 3, where the tessellations generated by Gibbs point processes are described. Several specific models are introduced. Section 4 comprises the main results of the paper. Firstly it recalls the general existence theorem of Gibbs measures, cf. [3]. This theorem is then applied in order to prove the existence of models introduced in Section 3. The uniqueness problem is beyond the scope of the present paper. Finally Section 5 contains simulations of Delaunay–Laguerre tessellations in a bounded window in 3D. Appendix gives a detailed description of pseudo-periodic configurations used to prove the existence of the tessellation models.

2. GEOMETRIC PRELIMINARIES

Motivation to this paper comes from modelling of materials microstructures, therefore we restrict ourselves to $\mathbb{R}^3$. Let $\mathcal{B}$ denote the Borel σ-algebra on $\mathbb{R}^3$ and the subset of $\mathcal{B}$ containing only bounded sets is denoted by $\mathcal{B}_b$. The symbol $B(c,r)$ denotes an open ball with center $c \in \mathbb{R}^3$ and radius $r \in \mathbb{R}$. Its boundary, the sphere with the center c and radius r, is denoted by $\partial B(c,r)$. Its closure is denoted by $\bar{B}(c,r)$. We will consider an interval of marks $S = [0, W]$, $W > 0$. Elements of $\mathbb{R}^3 \times S$ are called marked points and they are represented by a pair $x = (x', x'')$, with the location $x' \in \mathbb{R}^3$ and mark $x'' \in S$. In this paper, a letter with a prime refers to the point in $\mathbb{R}^3$ and the corresponding letter with double prime denotes the mark. The systems of locally finite marked point configurations and finite marked point configurations in $\mathbb{R}^3 \times S$ are denoted by $\mathbf{N}$ and $\mathbf{N}^f$, respectively. They are equipped with the σ-algebras

$$\mathcal{N} = \sigma(\{\mathbf{x} \in \mathbf{N} : \mathrm{card}(\mathbf{x}' \cap B) = n\} : B \in \mathcal{B}_b, n \in \mathbb{N}_0)$$

and $\mathcal{N}^f$ defined as the trace of $\mathbf{N}^f$ on $(\mathbf{N}, \mathcal{N})$. For a point configuration $\mathbf{x} \in \mathbf{N}$, we denote its positional part by $\mathbf{x}' = \{x' : (x', x'') \in \mathbf{x}\}$. The symbol η will always denote a finite subset of $\mathbf{x}$ and, analogously, η' its positional part. Throughout this text, $\Lambda \in \mathcal{B}_b$ will be the observation window. For configurations with points only on Λ, we use the notation $\mathbf{N}_\Lambda = \{\mathbf{x} \in \mathbf{N}^f : \mathbf{x}' \subset \Lambda\}$ and for $\mathbf{x} \in \mathbf{N}$ we write $\mathbf{x}_\Lambda = \{x \in \mathbf{x} : x' \in \Lambda\}$.

Finally, we say that a configuration $\mathbf{x}$ is in general position if

$$\eta \subset \mathbf{x}, 3 \leq \mathrm{card}(\eta) \leq 4 \Rightarrow \eta' \text{ is an affinely independent set of points in } \mathbb{R}^3. \quad (1)$$

We denote the system of all configurations in general position by $\mathbf{N}_{gp}$. Note that the

points $x'_0, \dots, x'_k \in \mathbb{R}^3$, $k \leq 3$, are affinely independent if the vectors $x'_1 - x'_0, \dots, x'_k - x'_0$ are linearly independent.

2.1. Power distance

For $\mathbf{x} \in \mathbf{N}$ and $x = (x', x'') \in \mathbf{x}$ the power distance [7] of a point $y' \in \mathbb{R}^3$ with respect to x is given by

$$\rho(y', x) = \|y' - x'\|^2 - x''. \tag{2}$$

If y' lies outside the ball $B(x', \sqrt{x''})$ the value $\rho(y', x)$ equals the squared length of the tangent line from y' to the sphere $\partial B(x', \sqrt{x''})$. The distance $\rho(y', x)$ equals 0 if y' lies on the sphere and it is smaller than 0 if y' lies inside the ball.

We say that two marked points p, q are orthogonal if $\rho(p', q) = p''$.

2.2. Delaunay–Laguerre tessellations

A tessellation [1] in $\mathbb{R}^3$ is a locally finite system of space-filling sets called cells which have mutually disjoint interiors. Many tessellations are determined by a point configuration, e. g., Voronoi tessellation [9]. Assume $\mathbf{x} \in \mathbf{N}$, then the Voronoi tessellation in $\mathbb{R}^3$ given by $\mathbf{x}'$ is a system of sets $\{w' \in \mathbb{R}^3 : ||w' - x'|| \leq ||w' - y'|| \ \forall y' \in \mathbf{x}'\}$, $x' \in \mathbf{x}'$. The points $\mathbf{x}'$ are called generators and we speak about the tessellation generated by the point pattern. Besides Voronoi tessellation, another example of a tessellation generated by a point pattern is Delaunay tessellation.

Assumption 1. In the rest of this section we will assume $\mathbf{x} \in \mathbf{N}_{gp}$, cf. (1). The assumption will be justified later in Section 3, Remark 3.1.

By symbol $B(\eta, \mathbf{x})$ we denote the ball such that $\eta' \subset \partial B(\eta, \mathbf{x})$ and call it circumball of η in $\mathbf{x}$. If such ball exists, we call η cospherical. In the case that $\mathrm{card}(\eta) = 4$, we use the symbol $\chi(\eta)$ for the diameter of the circumball and call it the circumdiameter. We say that $(\eta, \mathbf{x})$ satisfies the empty ball property if there exists a circumball $B(\eta, \mathbf{x})$ such that $B(\eta, \mathbf{x}) \cap \mathbf{x}' = \emptyset$. Assume that there are no $\eta \subset \mathbf{x}$ of cardinality > 4 being cospherical. The Delaunay tessellation in $\mathbb{R}^3$ given by $\mathbf{x}'$ is a system of sets $\{\mathrm{conv}(\eta') : \ \mathrm{card}(\eta') = 4, \ (\eta, \mathbf{x}) \text{ satisfies empty ball property}\}$, where conv is convex hull. The Delaunay tessellations of $\mathbb{R}^3$ are often called Delaunay tetrahedrizations, since their cells form tetrahedra.

Before proceeding to Laguerre Delaunay and Laguerre tessellations, we need to state some further properties of η and $\mathbf{x}$. We define the characteristic point of η as any marked point $p_\eta = (p'_\eta, p''_\eta) \in \mathbb{R}^3 \times \mathbb{R}$ which is orthogonal to every $x \in \eta$. If such p_η exists, we call η Laguerre-cospherical. Note that characteristic point p_η exists for all η with $\mathrm{card}(\eta) \leq 4$ and moreover p_η is unique whenever $\mathrm{card}(\eta) = 4$. We say that η is regular in $\mathbf{x}$ if $\rho(p'_\eta, y) \geq p''_\eta$ for all $y \in \mathbf{x}$. Note that the terms characteristic point, Laguerre cosphericity and regularity are extensions of the terms circumball, cosphericity and empty ball property, respectively.

We say that a configuration $\mathbf{x}$ is in reinforced general position if

$$\eta \subset \mathbf{x}, \mathrm{card}(\eta) > 4 \Rightarrow \eta \text{ is not Laguerre cospherical.} \tag{3}$$

We denote the system of all configurations in reinforced general position by $\mathbf{N}_{rgp}$.

Assumption 2. In the rest of this section we will assume $\mathbf{x} \in \mathbf{N}_{rgp}$, cf. (3). The assumption will be justified later in Section 3, Remark 3.1.

2.2.1. Laguerre–Delaunay tessellation

Having defined regularity, we can now define the following two sets. Let $\mathbf{x} \in \mathbf{N}$,

$$\mathcal{LD}(\mathbf{x}) := \{\eta \subset \mathbf{x} : \eta \text{ is regular}\}$$

and

$$\mathcal{LD}_k(\mathbf{x}) = \{\eta \in \mathcal{LD}(\mathbf{x}) : \mathrm{card}(\eta) = k\}, \text{ for } k = 1, \ldots, 4.$$

The Laguerre–Delaunay tessellation $LD(\mathbf{x})$ in $\mathbb{R}^3$ is then defined as a collection of tetrahedrons whose set of vertices is regular, i. e., collection of cells

$$D_\eta = (\mathrm{conv}(\eta'))_{\eta \in \mathcal{LD}_4(\mathbf{x})}\,.$$

2.2.2. Laguerre tessellation

The Laguerre tessellation $L(\mathbf{x})$ generated by a point pattern $\mathbf{x}$ is defined as a collection of nonempty cells given by

$$L_{x_i} = \{y' \in \mathbb{R}^3 : \rho(y', x_i) \leq \rho(y', x_j)\ \forall x_j \in \mathbf{x}, i \neq j\},\ x_i \in \mathbf{x}. \tag{4}$$

If one generator $y = (y', y'')$ lies inside the domain of another generator $x = (x', x'')$ (i. e., $y' \in B(x', \sqrt{x''})$) it can happen that either the cell corresponding to the generator y does not cover y' or even that there is no cell at all generated by y. In the latter case, it holds that $L(\mathbf{x}) = L(\mathbf{x} \setminus \{y\})$ and we say that y is redundant in $\mathbf{x}$.

2.2.3. Duality

The Laguerre and Laguerre Delaunay tessellations are dual, i. e., we can construct one if we know the other. Let $\mathcal{F}_0(L_x)$ denote the set of vertices of a nonempty cell L_x, $x \in \mathbf{x}$, $\mathbf{x} \in \mathbf{N}$. Then

$$\tilde{D}_v = \mathrm{conv}\{x' : x = (x', x'') \in \mathbf{x}, v \in \mathcal{F}_0(L_x)\}$$

is the Laguerre Delaunay cell of the vertex z. Let $\mathcal{F}_{0,\mathbf{x}} = \cup_{x \in \mathbf{x}} \mathcal{F}_0(L_x)$ denote the set of all vertices of the tessellation $L(\mathbf{x})$. The Laguerre Delaunay tessellation $LD(\mathbf{x})$ can then be alternatively defined as a collection of cells $\tilde{D}_v$, $v \in \mathcal{F}_{0,\mathbf{x}}$. For $x_1, x_2, x_3, x_4 \subset \mathbf{x}$ the set $\tilde{D}_v = \mathrm{conv}\{x_1, x_2, x_3, x_4\}$ is a Laguerre Delaunay cell if and only if $L_{x_1} \cap L_{x_2} \cap L_{x_3} \cap L_{x_4} \neq \emptyset$. It holds that $D_\eta = \tilde{D}_v$ if $\eta = \{x \in \mathbf{x} : v \in \mathcal{F}_0(L_x)\}$.

2.2.4. Reduction

In the case that all marks are equal, the Laguerre tessellation reduces to a Voronoi tessellation and the Laguerre Delaunay tessellation reduces to Delaunay tessellation. The regularity property becomes the empty ball property. To see this assume $\mathbf{x}$ be a marked point configuration with all marks equal to zero. Then for any $\eta \subset \mathbf{x}$ with $\mathrm{card}(\eta) = 4$

the ball $B(p'_\eta, \sqrt{p''_\eta})$ becomes precisely $B(\eta, \mathbf{x})$, the circumball of η. Therefore η is regular if and only if η satisfies the empty ball property. Finally note that the tessellation is invariant under any translation of marks such that the new marks still lie in $[0, W]$.

Similarly to [4], where both Voronoi and Delaunay tessellations are unified into one tessellation class called Delaunay–Voronoi tessellations, we will consider class of Delaunay–Laguerre tessellations to be the union of Laguerre tessellations and their duals Laguerre Delaunay tessellations.

2.3. Hypergraphs

In this section, we follow the usage of hypergraphs from [3]. The concept of hypergraph is mainly the theoretical tool how to effectively describe the tessellation geometry.

A hypergraph structure is a measurable subset $\mathcal{E}$ of $(\mathbf{N}^f \times \mathbf{N}, \mathcal{N}^f \otimes \mathcal{N})$ such that $\eta \subset \mathbf{x}$ for all $(\eta, \mathbf{x}) \in \mathcal{E}$. We call η a hyperedge of $\mathbf{x}$ and write $\eta \in \mathcal{E}(\mathbf{x})$, where $\mathcal{E}(\mathbf{x}) = \{\eta : (\eta, \mathbf{x}) \in \mathcal{E}\}$. For a given $\mathbf{x} \in \mathbf{N}$, the pair $(\mathbf{x}, \mathcal{E}(\mathbf{x}))$ is called a hypergraph.

Notice that we have already defined five hypergraph structures. Indeed, for $\mathbf{x} \in \mathbf{N}$, the pairs $(\mathbf{x}, \mathcal{LD}(\mathbf{x}))$ and $(\mathbf{x}, \mathcal{LD}_k(\mathbf{x}))$, $k = 1, \dots, 4$, are hypergraphs.

The finite point configuration η, $\mathrm{card}(\eta) = k$, is said to be connected in $\mathcal{LD}(\mathbf{x})$ if for any two points $x, y \in \eta$ there exists a path between x and y in the graph $\mathcal{LD}_2(\mathbf{x})$, that is, there exists $m \in \{1, \dots, k-1\}$ and a sequence $x_0, \dots, x_m \in \eta$ such that $x = x_0$, $y = x_m$ and

$$\{x_i, x_{i+1}\} \in \mathcal{LD}_2(\mathbf{x})$$

for all $i \in \{0, \dots, m-1\}$.

We define the graph of connected k-tuples

$$\mathcal{CG}_k = \{(\eta, \mathbf{x}) : \eta \subset \mathbf{x}, \mathrm{card}(\eta) = k, \eta \text{ is connected in } \mathcal{LD}(\mathbf{x})\}$$

and

$$\mathcal{CG}_{k,b} = \{(\eta, \mathbf{x}) \in \mathcal{CG}_k : \forall x \in \eta : L_x \text{ is bounded}\}.$$

Both $\mathcal{CG}_k$ and $\mathcal{CG}_{k,b}$ are hypergraph structures.

A hyperedge potential is a measurable function $\varphi : \mathcal{E} \to \mathbb{R} \cup \{+\infty\}$. For notational convenience, we set $\varphi = 0$ on $\mathcal{E}^c$. The function φ introduces interactions on hyperedges that need not be hereditary since φ is allowed to take the value ∞ (hard-core case). The hyperedge potential is said to be hereditary if $\varphi(\eta, \mathbf{x}) < \infty$ for some $(\eta, \mathbf{x}) \in \mathcal{E}$ implies that $\varphi(\eta, \tilde{\mathbf{x}}) < \infty$ for all $\tilde{\mathbf{x}} \subset \mathbf{x}$ such that $\eta \in \mathcal{E}(\tilde{\mathbf{x}})$.

Hyperedge potential is shift-invariant if

$$(\vartheta_t \eta, \vartheta_t \mathbf{x}) \in \mathcal{E} \text{ and } \varphi(\vartheta_t \eta, \vartheta_t \mathbf{x}) = \varphi(\eta, \mathbf{x}) \text{ for all } (\eta, \mathbf{x}) \in \mathcal{E} \text{ and } t \in \mathbb{R},$$

where $\vartheta_t \mathbf{x} = \{(x', x'') \in \mathbb{R}^3 \times S : (x' + x, x'') \in \mathbf{x}\}$ is the translation of the positional part of the configurations by the vector $-t \in \mathbb{R}^3$. All hyperedge potentials mentioned in this paper are assumed to be shift-invariant.

A hyperedge potential φ is unary for the hypergraph structure $\mathcal{E}$ if there exists a measurable function $\hat{\varphi} : \mathbf{N} \to \mathbb{R} \cup \{+\infty\}$ such that

$$\varphi(\eta, \mathbf{x}) = \hat{\varphi}(\eta) \text{ for } \eta \in \mathcal{E}(\mathbf{x}).$$

A set $\Delta \in \mathcal{B}_b$ is a finite horizon for the pair $(\eta, \mathbf{x}) \in \mathcal{E}$ and the hyperedge potential φ if for all $\tilde{\mathbf{x}} \in \mathbf{N}, \tilde{\mathbf{x}} = \mathbf{x}$ on $\Delta \times S$

$$(\eta, \tilde{\mathbf{x}}) \in \mathcal{E} \text{ and } \varphi(\eta, \tilde{\mathbf{x}}) = \varphi(\eta, \mathbf{x}).$$

Remark 2.1. (Finite horizon in case of $\mathcal{LD}$ and unary potential)
Let $\eta \in \mathcal{LD}(\mathbf{x})$ and p_η is its characteristic point. The ball $B(p'_\eta, \sqrt{p''_\eta})$ does not contain the points of η. To see this, take two points x, y with $x'', y'' > 0$ such that they are orthogonal, i. e., $\rho(x', y) = x''$. Then $y'' = \rho(y', x) < \|y' - x'\|^2$ and thus $\sqrt{y''} < \|y' - x'\|$. The goal is to construct a finite horizon for a given pair $(\eta, \mathbf{x}) \in \mathcal{LD}$ and a given unary potential. Notice that the finite horizon does not depend on the unary potential, since $\varphi(\eta, \tilde{\mathbf{x}}) = \hat{\varphi}(\eta) = \varphi(\eta, \mathbf{x})$ for $\hat{\varphi}$ from the definition of the unary potential. Therefore, all we need to fulfill is that $(\eta, \tilde{\mathbf{x}}) \in \mathcal{E}$ for every $\tilde{\mathbf{x}} \in \mathbf{N} : \tilde{\mathbf{x}} = \mathbf{x}$ on $\Delta \times S$. To do that we use the fact that the mark space is bounded, $S = [0, W]$. Then $\Delta = B(p'_\eta, \sqrt{p''_\eta + W})$ is sufficient as a horizon, since any point $w = (w', w'') \in (\mathbb{R}^3 \setminus \Delta) \times S$ satisfies $\|p'_\eta - w'\| \geq \sqrt{p''_\eta + W}$ and therefore cannot violate the regularity of η. Indeed, since $w'' \leq W$, $\|p'_\eta - w'\| \geq \sqrt{p''_\eta + w''}$, what means that η is regular in arbitrary $\tilde{\mathbf{x}} \in \mathbf{N} : \tilde{\mathbf{x}} = \mathbf{x}$ on $\Delta \times S$. Moreover all points of η' are contained in the set Δ, since for every $w \in \eta$ we have $\|p'_\eta - w'\| = \sqrt{p''_\eta + w''} \leq \sqrt{p''_\eta + W}$. The set $\Delta \setminus B(p'_\eta, \sqrt{p''_\eta})$ is an annulus with width $\sqrt{p''_\eta + W} - \sqrt{p''_\eta} = \frac{W}{\sqrt{p''_\eta + W} + \sqrt{p''_\eta}} \leq \sqrt{W}$. Although the number of points in the annulus is not bounded, we have the bound on its width.

Let $\Lambda \in \mathcal{B}_b$. Define the set

$$\mathcal{E}_\Lambda(\mathbf{x}) := \{\eta \in \mathcal{E}(\mathbf{x}) : \varphi(\eta, \zeta \cup \mathbf{x}_{\Lambda^c}) \neq \varphi(\eta, \mathbf{x}) \text{ for some } \zeta \in \mathbf{N}_\Lambda\}.$$

Let $\Lambda \in \mathcal{B}_b$ be given. We say a configuration $\mathbf{x} \in \mathbf{N}$ confines the range of φ from Λ if there exists a set $\partial\Lambda(\mathbf{x}) \in \mathcal{B}_b$ such that $\varphi(\eta, \zeta \cup \tilde{\mathbf{x}}_{\Lambda^c}) = \varphi(\eta, \zeta \cup \mathbf{x}_{\Lambda^c})$ whenever $\tilde{\mathbf{x}} = \mathbf{x}$ on $\partial\Lambda(\mathbf{x}) \times S$, $\zeta \in \mathbf{N}_\Lambda$ and $\eta \in \mathcal{E}_\Lambda(\zeta \cup \mathbf{x}_{\Lambda^c})$. In this case we write $\mathbf{x} \in \mathbf{N}_{\mathrm{cr}}^\Lambda$. We denote $r_{\Lambda,\mathbf{x}}$ the smallest possible r such that $(\Lambda + B(0, r)) \setminus \Lambda$ satisfies the definition of $\partial\Lambda(\mathbf{x})$. We will use the abbreviation $\partial_\Lambda \mathbf{x} = \mathbf{x}_{\partial\Lambda(\mathbf{x})}$.

3. RANDOM POINT PROCESSES AND TESSELLATIONS

In this section we present the theory concerning Gibbs point processes defined by an energy function. The energy function can be viewed as a sum of functions called potentials. Viewing the realization of a Gibbs point process as a point configuration of generators of Delaunay–Laguerre tessellations, introduced in Subsection 2.2, results in random tessellations. Finally, several choices of the energy function will be introduced in order to be used later in the following sections.

3.1. Gibbs point processes

Let π^z be the distribution of a homogeneous Poisson point process on $\mathbb{R}^3 \times S$ with intensity measure $\nu = z\lambda \times \mu$, $z > 0$, where λ is the Lebesgue measure on $\mathbb{R}^3$ and μ is the Lebesgue measure on S, serving as a reference measure. The parameter z is called the intensity. We will shorten $\pi = \pi^1$. We set π^z_Λ to be the distribution of a marked Poisson point process with intensity measure ν restricted to $\Lambda \times S$.

Remark 3.1. (General position)
In Section 2 we assumed $\mathbf{x} \in \mathbf{N}_{gp}$ (Assumption 1) and subsequently also $\mathbf{x} \in \mathbf{N}_{rgp}$ (Assumption 2). These assumptions are not restrictive, as both $\mathbf{N}_{gp}$ and $\mathbf{N}_{rgp}$ are measurable and for any $\Lambda \in \mathcal{B}_b$ it holds that $\pi^z_\Lambda(\mathbf{N} \setminus \mathbf{N}_{gp}) = \pi^z_\Lambda(\mathbf{N} \setminus \mathbf{N}_{rgp}) = 0$, see [16].

The energy function is a measurable function $E : \mathbf{N}^f \longrightarrow \mathbb{R} \cup \{+\infty\}$. In general, it can be expressed (resembling the definition of Hamiltonian below) as a sum of values of the hyperedge potential φ over hyperedges of some hypergraph structure $\mathcal{E}$, i. e.,

$$E(\mathbf{x}) = \sum_{\eta \in \mathcal{E}(\mathbf{x})} \varphi(\eta, \mathbf{x}) \text{ for } \mathbf{x} \in \mathbf{N}_f.$$

We will consider it to be nondegenerate, i. e., $E(\emptyset) < +\infty$.

Considering $\mathbf{x} \in \mathbf{N}$ and taking $\xi \in \mathbf{N}_\Lambda$ we define the energy (Hamiltonian) of ξ in Λ with boundary condition $\mathbf{x}$ by the formula

$$E_{\Lambda,\mathbf{x}}(\xi) = \sum_{\eta \in \mathcal{E}_\Lambda(\xi \cup \mathbf{x}_{\Lambda^c})} \varphi(\eta, \xi \cup \mathbf{x}_{\Lambda^c}), \tag{5}$$

provided the sum is well-defined (i. e., the negative part is finite, $E^-_{\Lambda,\mathbf{x}}(\xi) < \infty$). In the case $\xi = \mathbf{x}_\Lambda$ we write $E_{\Lambda,\mathbf{x}}(\mathbf{x}_\Lambda) = E_\Lambda(\mathbf{x})$ and speak about the local energy of $\mathbf{x}$ in Λ. It is the energetic contribution of points $\mathbf{x}_\Lambda$ in the computation of the energy of $\mathbf{x}$.

The infinite Gibbs point process with activity z and energy function E is a point process with distribution Φ (called stationary Gibbs measure) having conditional densities with respect to π_Λ of the form

$$f(\mathbf{x}_\Lambda, \mathbf{x}_{\Lambda^c}) = \frac{1}{Z_\Lambda(\mathbf{x}_{\Lambda^c})} z^{\mathrm{card}(\mathbf{x}_\Lambda)} \exp\left(-E_\Lambda(\mathbf{x})\right) \text{ for every } \Lambda \in \mathcal{B}_b(\mathbb{R}^3) \text{ and for } \Phi{-}a.a.\ \mathbf{x}_{\Lambda^c}, \tag{6}$$

where

$$Z_\Lambda(\mathbf{x}_{\Lambda^c}) = \int z^{\mathrm{card}(\mathbf{x}_\Lambda)} \exp\left(-E_\Lambda(\mathbf{x})\right) \pi_\Lambda(\mathrm{d}\mathbf{x}_\Lambda)$$

is the normalizing constant called partition function and the argument indicates its dependence on $\mathbf{x}_{\Lambda^c}$.

First, some conditions on the energies E_Λ have to be stated in order to ensure that the conditional densities are well-defined. A configuration $\mathbf{x} \in \mathbf{N}$ is called admissible for a region Λ and an activity $z > 0$ if $E^-_{\Lambda,\mathbf{x}}(\xi) < \infty$ for π_Λ-a.a. $\xi \in \mathbf{N}_\Lambda$ (i. e., $E_{\Lambda,\mathbf{x}}$ is almost surely well-defined) and $0 < Z_\Lambda(\mathbf{x}_{\Lambda^c}) < \infty$. The stationary Gibbs measure is concentrated on the set of admissible configurations for all $\Lambda \in \mathcal{B}_b$. The extension of the energy function from finite point configurations to all locally finite configurations is required in (6). This can be achieved if a configuration $\mathbf{x}$ confines the range of φ from Λ, i. e., $\mathbf{x} \in \mathbf{N}^\Lambda_{cr}$, then

$$E_{\Lambda,\mathbf{x}}(\xi) = \sum_{\eta \in \mathcal{E}_\Lambda(\xi \cup \partial_\Lambda \mathbf{x})} \varphi(\eta, \xi \cup \mathbf{x}_{\Lambda^c}).$$

Even in the case when conditional densities are well-defined the existence of stationary Gibbs point process is not obvious and the entire Section 4 will be devoted to this problem.

3.2. Random Gibbs-type tessellations

Considering the generators of Delaunay–Laguerre tessellations to be a Gibbs point process gives us the appropriate random tessellations that are of the interest of this paper. The energy function depending on the tessellation geometry will be considered. Later in Section 4 the existence results of infinite Gibbs point processes for particular choices of the energy function will be established. On the other hand for the purposes of simulations in Section 5 only finite Gibbs point processes are needed, since the simulations are exercised only on a bounded observation window. For a description of a 3D tessellation, the m-dimensional facets, $m = 0, 1, 2, 3$, are used, namely the vertices, edges, faces, and cells, respectively.

Recall that the energy function E is built as a sum of functions φ called potentials over hyperedges of some hypergraph structure $\mathcal{E}$, cf. (5). We will distinguish two types of potential functions. If the potential attains only finite values we speak about soft-core potential or smooth interaction. Conversely, the potential or interaction is called hard-core if it can attain the value $+\infty$.

The existence of an infinite Gibbs-type models will be treated in Section 4 for the following choices of potentials and hypergraph structures.

1. Soft-core unary potential that is nonnegative and at most polynomially increasing with respect to the circumdiameter, i. e.

$$\varphi_S(\eta, \mathbf{x}) \leq K_0 + K_1 \chi(\eta)^\beta, \ \eta \in \mathcal{LD}_4(\mathbf{x}),$$

for some $K_0, K_1 \geq 0, \beta > 0$.

2. Hard-core unary potential such that

$$\sup_{\eta: d_0 \leq \chi(\eta) \leq d_1} \varphi_{HC}(\eta, \mathbf{x}) < \infty \text{ and } \varphi_{HC}(\eta, \mathbf{x}) = \infty \text{ if } \chi(\eta) > \alpha, \ \eta \in \mathcal{LD}_4(\mathbf{x}),$$

for some $0 \leq d_0 < d_1 \leq \alpha$.

3. Soft-core pair potential defined for two Laguerre cells having a common face

$$\varphi_{2,\mathrm{NVR}}(\eta, \mathbf{x}) = \mathrm{NVR}(L_{x_1}, L_{x_2}) \wedge K, \ \eta = \{x_1, x_2\} \in \mathcal{LD}_2(\mathbf{x}), \tag{7}$$

where $K > 0$ and neighbour-volume ratio NVR is defined by

$$\mathrm{NVR}(L_{x_1}, L_{x_2}) = \left(\frac{\max\{\mathrm{vol}(L_{x_1}), \mathrm{vol}(L_{x_2})\}}{\min\{\mathrm{vol}(L_{x_1}), \mathrm{vol}(L_{x_2})\}} - 1 \right)^{1/2}, \tag{8}$$

where $\mathrm{vol}(L)$ is the volume of a cell L. The potential given in (7) may be multiplied by a real parameter θ. In such case, the sign of θ is crucial. In the case of $\theta > 0$, the neighbouring cells are forced to have a similar volume, while $\theta < 0$ forces the neighbouring cells to have different volumes. The choice of the power $1/2$, in (8) and later in (9), has proven itself useful in practice, but in general the power can be chosen arbitrarily.

4. Soft-core reconstructing potential

$$\varphi^{s}_{k,T}(\eta, \mathbf{x}) = (|T(s(\{L_x : x \in \eta\})) - s_0|)^{1/2} \wedge K,\ \eta \in \mathcal{CG}_{k,b}(\mathbf{x}), \tag{9}$$

where $K > 0$, $k \in \mathbb{N}$. The symbol s represents a univariate geometric characteristic of a single cell, e. g., volume of a cell, number of faces per cell, etc. Let the same symbol with arguments $s(L_1, \ldots, L_k)$ denote a sample of k values of the geometric characteristic assigned to a collection of cells $L_1, \ldots, L_k$, formally $s : \mathcal{C}^k \to \mathbb{R}^k$, where $\mathcal{C}$ is the system of all convex polygons in $\mathbb{R}^3$. The functional $T : \mathbb{R}^k \to \mathbb{R}$ comprises the sample into a real value. Finally, $s_0 \in \mathbb{R}$ is the value we want the $T(s(\cdot))$ to reach. For example $T(s(\cdot)) = \bar{s}(\cdot)$ and $T(s(\cdot)) = s^2(\cdot)$ stand for the sample mean and sample variance, respectively, computed over the cells in the argument. These potentials allow us to control the moments of some geometric characteristic on the k-tuples of cells.

A further possibility is to control the entire distribution of the geometric characteristic s. Let $H_{s(L_1,\ldots,L_k)}$ be the histogram of the geometric characteristic s computed from cells $L_1, \ldots, L_k$. Let H'_s be the prescribed targeting histogram of s that we want to approach (this can be typically obtained from data). We want the potential to measure the level of similarity between histograms $H_{s(\cdot)}, H'_s$. To this purpose we define the discrepancy of two histograms below.

Remark 3.2. (Scope of geometric characteristics)
In (9) a geometric characteristic s of a single cell was considered for simplicity. In general, instead of a single cell we can consider a m-dimensional facet, $m = 0, 1, \ldots, d$, where d is the dimension, in our case $d = 3$. E.g., in the case of $m = 2$ we obtain faces of cells and $s = \mathrm{NVR}$ is an example of face characteristic. Then $s((L_{1,1}, L_{2,1}), \ldots, (L_{1,k}, L_{2,k}))$ denotes the sample of k NVR values, $s : \mathcal{C}^{(d+1-m)k} \to \mathbb{R}^k$. We say that n-tuple of points $x_1, \ldots, x_n$ is mutually connected if $\{x_i, x_j\} \in \mathcal{LD}_2(\mathbf{x})$ for all $i, j \in 1, \ldots, n$. The graph of connected k-tuples $\mathcal{CG}_k$ has to be modified into $\{(\eta, \mathbf{x}) : \eta \subset \mathbf{x}, \eta$ is connected in $\mathcal{LD}(\mathbf{x})$, η contains k mutually connected $(d + 1 - m)$-tuples$\}$.

Histogram discrepancy: Let us consider a geometric characteristic s of the m-dimensional facets, $m = 0, 1, 2, 3$, attaining values on an interval $[a, b]$. For an integer I let $D = \{t_i\}_{i=0}^{I}$ be a partition of the interval such that $t_0 = a$ and $t_I = b$ (D does not need to be equidistant). The histogram $H_{s(\cdot)}$ can then be represented by some numbers $h_1, \ldots, h_I$ interpreted as frequencies of the classes $1, \ldots, I$ (i. e., h_i is the number of facets for which the value of the considered geometric characteristic lies in the interval $[t_{i-1}, t_i)$). We use the abbreviating notation $P = \sum_{i=1}^{I} h_i$. The discrepancy for a pair of histograms $(H_{s(\cdot)}, H'_s)$ on the same interval and with the same bins (this implies the same number of classes) can then be written as

$$\mathrm{dsc}(H_{s(\cdot)}, H'_s) = \sum_{i=1}^{I} \left| \frac{h_i}{P} - \frac{h'_i}{P'} \right|. \tag{10}$$

The discrepancy dsc measures the difference between two histograms and is minimized when they are identical up to some positive multiplicative constant (i. e., that there exists a constant J such that $h_i = Jh'_i$ for every $i = 1, \ldots, I$).

The choice $T(s(\cdot)) = \mathrm{dsc}(H_{s(\cdot)}, H'_s)$ enables us to control the entire distribution of the geometric characteristic s.

4. EXISTENCE

Having in mind the definition of infinite Gibbs point processes we proceed to another main issue of this paper, to prove the existence of particular Gibbs measures specified by four potentials stated at the end of the Subsection 3.2. First of all we present the main existence theorem from [3] together with the conditions we need. Further in the next two subsections we verify the assumptions of the existence theorem and show for which values of the activity parameter the measures defined by potentials in 3.2 exist.

4.1. Assumptions and existence theorem

Firstly we state three assumptions from [3] which are sufficient for the existence of a Gibbs measure, cf. Theorem 4.1.

(R) *The range condition.* There exist constants $\ell_R, n_R \in \mathbb{N}$ and $\delta_R < \infty$ such that for all $(\eta, \mathbf{x}) \in \mathcal{E}$ one can find a finite horizon Δ satisfying: For every $x, y \in \Delta$ there exist ℓ open balls $B_1, \ldots, B_\ell$ (with $\ell \leq \ell_R$) such that

- the set $\cup_{i=1}^{\ell} \bar{B}_i$ is connected and contains x and y, and
- for each i, either $\mathrm{diam}(B_i) \leq \delta_R$ or $\mathrm{card}(\mathbf{x} \cap B_i) \leq n_R$.

(S) *Stability.* The energy function E is called *stable* if there exists a constant $c_S \geq 0$ such that

$$E_{\Lambda,\mathbf{x}}(\zeta) \geq -c_S \cdot \mathrm{card}(\zeta \cup \partial_\Lambda \mathbf{x})$$

for all $\Lambda \in \mathcal{B}_b$, $\zeta \in \mathbf{N}_\Lambda$ and $\mathbf{x} \in \mathbf{N}^\Lambda_{\mathrm{cr}}$.

(U) *Upper regularity.* M and Γ, cf. Subsection (A.1), can be chosen so that the following holds.

(U1) *Uniform confinement*: $\bar{\Gamma} \subset \mathbf{N}^\Lambda_{\mathrm{cr}}$ for all $\Lambda \in \mathcal{B}_b$ and

$$r_\Gamma := \sup_{\Lambda \in \mathcal{B}_b(\mathbb{R}^3)} \sup_{\mathbf{x} \in \bar{\Gamma}} r_{\Lambda,\mathbf{x}} < \infty, \tag{11}$$

where $r_{\Lambda,\mathbf{x}}$ was defined in (2.3) below the Remark (2.1).

(U2) *Uniform summability*:

$$c^+_\Gamma := \sup_{\mathbf{x} \in \bar{\Gamma}} \sum_{\eta \in \mathcal{E}(\mathbf{x}) : \eta' \cap C \neq \emptyset} \frac{\varphi^+(\eta, \mathbf{x})}{\mathrm{card}(\hat{\eta})} < \infty,$$

where $\hat{\eta} := \{k \in \mathbb{Z}^3 : \eta' \cap C(k) \neq \emptyset\}$ and φ^+ is the positive part of φ.

(U3) *Strong non-rigidity*: $e^{z|C|}\pi^z_C(\Gamma) > e^{c_\Gamma}$, where c_Γ is defined as in (U2) with φ in place of φ^+.

($\hat{\mathbf{U}}$) *Alternative upper regularity.* M and Γ can be chosen so that the following holds.

($\hat{\text{U}}1$) *Lower density bound*: There exist constants $c, d > 0$ such that

$$\text{card}(\zeta) \geq c|\Lambda| - d$$

whenever $\zeta \in \mathbf{N}_f \cap \mathbf{N}_\Lambda$ is such that $E_{\Lambda,\mathbf{x}}(\zeta) < \infty$ for some $\Lambda \in \mathcal{B}_b$ and some $\mathbf{x} \in \bar{\Gamma}$.

($\hat{\text{U}}2$) = (U2) *Uniform summability.*

($\hat{\text{U}}3$) *Weak non-rigidity*: $\Pi^z_C(\Gamma) > 0$.

Theorem 4.1. For every hypergraph structure $\mathcal{E}$, hyperedge potential φ and activity $z > 0$ satisfying **(S)**, **(R)** and **(U)** there exists at least one Gibbs measure.

Alternate version of the theorem is obtained by replacing the condition **(U)** by **($\hat{\text{U}}$)**.

Theorem 4.2. A Gibbs measure exists also under the assumptions **(S)**, **(R)** and **($\hat{\text{U}}$)**.

The proof of both theorems can be found in [3], see Theorems 3.2 and 3.3 together with Remark 3.7.

The fact that the hypergraph structure possesses a type of locality property is crucial for the existence of Gibbs measures. The first assumption **(R)** reflects this requirement. It says that hyperedges with a large horizon require the existence of a large ball with only a few points. It implies that the energy function $E_{\Lambda,\mathbf{x}}$ depends only on the points of $\mathbf{x}$ in a bounded set $\partial\Lambda(\mathbf{x})$. Further it justifies the restriction on $\mathbf{N}^\Lambda_{\text{cr}}$ since any translation-invariant locally finite counting measure is concentrated on the set $\mathbf{N}^\Lambda_{\text{cr}}$, see Proposition 3.1. in [3]. If all horizon sets can be chosen to have uniformly bounded diameters, the range condition is trivially satisfied. The stability assumption **(S)** ensures the finiteness of all normalizing constants $Z_\Lambda(\mathbf{x}_{\Lambda^c})$ in (6).

Remark 4.3. (Stability condition)
Stability is trivially satisfied if φ is non-negative, then **(S)** holds with $c_S = 0$. In case that the hyperedge potential is bounded below, i. e., $\varphi(\eta, \mathbf{x}) \geq -c_\varphi$ for some $c_\varphi < \infty$, stability is ensured if the hypergraph $\mathcal{E}$ is sublinear, i. e., if $\exists C < \infty : \forall \mathbf{x} \in \mathbf{N}_f :$ $\text{card}(\mathcal{E}(\mathbf{x})) \leq C \cdot \text{card}(\mathbf{x})$.

Finally, when verifying the upper regularity conditions **(U)**, we can restrict ourselves only on the so called pseudo-periodic configurations defined in Appendix A. The assumption (U1) states that the pseudo-periodic configurations in $\bar{\Gamma}$ confine the range of φ in a uniform way. Condition (U2) provides a uniform upper bound for the local energy $E_{\Lambda,\cdot}$ on $\bar{\Gamma}$. The last condition (U3) is satisfied for all $z \geq z_0$ for some $z_0 \geq 0$, provided that (U2) holds and $\pi^z_C(\Gamma) > 0$. The alteration **($\hat{\text{U}}$)** can help us when it is difficult to satisfy (U3) for small values of z.

Remark 4.4. (Simplification of the upper regularity condition)
Using the set Γ^A, defined in Subsection A.1, the conditions (U2) and (U3) can be simplified. In (U2), $\text{card}(\hat{\eta}) = \text{card}(\eta)$ since each point of η is in a different set $C(k)$. In (U3), $\pi^z_C(\Gamma)$ can be directly calculated:

$$\pi^z_C(\Gamma^A) = \pi^z_C(\{\xi \in \mathbf{N}_C : \xi = \{p\}, p \in A\}) = e^{-z|A|} z|A| e^{-z|C\setminus A|} = e^{-z|C|} z|A|.$$

(U3) is then of the form $z|A| > e^{C_\Gamma}$. By taking A as in (15) one obtains

$$|A| = \frac{4}{3}\pi\rho^3 a^3 \cdot \left(\frac{a}{2}(1-2\rho)\right)^2 = \frac{1}{3}\pi a^5 \rho^3 (1-2\rho)^2.$$

4.2. Auxiliary lemmas

In the following two subsections, we prove the existence of four different models. Some elements of the proofs are common to all theorems and thus are included here as auxiliary lemmas.

The first lemma states that uniformly bounded finite horizons imply uniform confinement (U1).

Lemma 4.5. Let $\Gamma \subset \mathbf{N}$ be a class of configurations. If there exists $d_{\max} > 0$ such that $\mathrm{diam}\Delta < d_{\max}$ for the horizon Δ of any $(\eta, \mathbf{x}), \eta \in \mathcal{E}(\mathbf{x}), \mathbf{x} \in \Gamma$, then

$$r_\Gamma < d_{\max},$$

where r_Γ is defined as in the condition $(U1)$.

Proof. Choose $\Lambda \in \mathcal{B}_b$ and $\mathbf{x} \in \Gamma$. Let $\zeta \in \mathbf{N}_\Lambda$, $\eta \in \mathcal{E}_\Lambda(\zeta \cup \mathbf{x}_{\Lambda^c})$ and denote Δ the finite horizon of $(\eta, \mathbf{x})$. Then $\Delta \cap \Lambda \neq \emptyset$, since

$$\eta \in \mathcal{E}_\Lambda(\zeta \cup \mathbf{x}_{\Lambda^c}) \Leftrightarrow \exists \xi \in \mathbf{N}_\Lambda : \varphi(\eta, \zeta \cup \mathbf{x}_{\Lambda^c}) \neq \varphi(\eta, \xi \cup \mathbf{x}_{\Lambda^c})$$

$$\Rightarrow \exists \xi \in \mathbf{N}_\Lambda : \xi' \cap \Delta \neq \emptyset \Rightarrow \Lambda \cap \Delta \neq \emptyset.$$

Therefore $\Delta \subset \Lambda + B(0, d_{\max})$. If we take $\tilde{\mathbf{x}} \in \Gamma$ such that $\tilde{\mathbf{x}} = \mathbf{x}$ on $\partial\Lambda(\mathbf{x})$ then $\varphi(\eta, \zeta \cup \mathbf{x}_{\Lambda^c}) = \varphi(\eta, \zeta \cup \tilde{\mathbf{x}}_{\Lambda^c})$ since $\zeta \cup \mathbf{x}_{\Lambda^c}$ and $\zeta \cup \tilde{\mathbf{x}}_{\Lambda^c}$ differ only on Δ^c. □

Lemma 4.6. For models with the hypergraph structure $\mathcal{LD}$ or $\mathcal{LD}_k$, k=1,...,4, with a unary potential, the range condition is satisfied with parameters $\ell_R = 3, n_R = 0, \delta_R = 2\sqrt{W}$.

Proof. Take the horizon set $\Delta = B(p'_\eta, \sqrt{p''_\eta + W})$. As described in Remark 2.1, Δ can be decomposed into the ball $B(p'_\eta, \sqrt{p''_\eta})$ and $\Delta \setminus B(p'_\eta, \sqrt{p''_\eta})$, a 3-dimensional annulus with width

$$\sqrt{p''_\eta + W} - \sqrt{p''_\eta} = W / \left(\sqrt{p''_\eta + W} + \sqrt{p''_\eta}\right).$$

The ball $B(p'_\eta, \sqrt{p''_\eta})$ determined by the characteristic point p_η cannot contain any points of $\mathbf{x}$. Although the annulus $\Delta \setminus B(p'_\eta, \sqrt{p''_\eta})$ does not have any bound on the number of points, its width is bounded by $\sqrt{W}$. This means that any $x, y \in \Delta$ can be connected by the spheres $B(x, \sqrt{W}), p_\eta, B(y, \sqrt{W})$, yielding the parameters $\ell_R = 3, n_R = 0, \delta_R = 2\sqrt{W}$. □

4.3. Tetrahedrization models

We now prove the existence for two Laguerre Delaunay models.

Proposition 4.7. There exists at least one Gibbs measure for the model $(\mathcal{LD}_4, \varphi_S)$ and every activity

$$z > \frac{3}{4\pi} e^{8K_0} \left(\frac{2K_1 \beta e}{5} \right)^{\frac{5}{\beta}} \frac{(\chi_1(\rho)^\beta + 3\chi_2(\rho)^\beta)^{\frac{5}{\beta}}}{\rho^3 (1-2\rho)^2}. \tag{12}$$

Proof.

(R) The range condition is proven in Lemma 4.6.

(S) Stability is satisfied because φ is non-negative, see Remark 4.3.

(U) We choose M and Γ as in Subsubsection A.1.

(U1) By Remark A.4 there is $R_0 > 0$ such that $p''_\eta \leq R_0$ for all $\eta \in \mathcal{LD}_4(\mathbf{x}), \mathbf{x} \in \bar{\Gamma}^A$. For $(\eta, \mathbf{x}) \in \mathcal{LD}$ and a unary potential the finite horizon can be taken as $\Delta = B(p'_\eta, \sqrt{p''_\eta + W})$, cf. Remark 2.1. Together we have $\operatorname{diam} \Delta = 2\sqrt{p''_\eta + W} \leq 2\sqrt{R_0 + W}$. By Lemma 4.5 we have $r_\Gamma \leq \sqrt{R_0 + W}$.

(U2) c^+_Γ is finite since the number of summands is $n_T \leq 32$, cf. Remark A.2, and φ_S is bounded thanks to the Remark A.3.

(U3) Using the simplification from Remark 4.4, we obtain

$$z > \frac{1}{|A|} e^{C_\Gamma} = \frac{3}{4\pi\rho^3 a^5 (1-2\rho)^2} e^{C_\Gamma},$$

where $|A| = \frac{4}{3}\pi\rho^3 a^5 (1-2\rho)^2$ thanks to Remark A.1.

$$c_\Gamma = \sup_{\mathbf{x} \in \bar{\Gamma}} \sum_{\eta \in \mathcal{LD}_4(\mathbf{x}) : \eta' \cap C \neq \emptyset} \frac{\varphi(\eta, \mathbf{x})}{\operatorname{card}(\hat{\eta})} \leq \sum_{\eta \in \mathcal{LD}_4(\mathbf{x}) : \eta' \cap C \neq \emptyset} \frac{K_0 + K_1 \chi(\eta)^\beta}{4} =$$

where $\varphi(\eta, \mathbf{x}) \leq K_0 + K_1 \chi(\eta)^\beta$ and $\operatorname{card}(\hat{\eta}) = 4$,

$$= 8\frac{K_0 + K_1\chi(\eta)^\beta}{4} + 24\frac{K_0 + K_1\chi(\eta)^\beta}{4} \leq 2(K_0 + K_1(a\chi_1)^\beta) + 6(K_0 + K_1(a\chi_2)^\beta) =$$

since the number of summands is $n_T \leq 32$ and it splits to 8 tetrahedra T_1 and 24 tetrahedra T_2, cf. Remark A.2 and Figure 9. The circumdiameters are bounded thanks to the Remark A.3,

$$= 8K_0 + 2K_1((a\chi_1)^\beta + 3(a\chi_2)^\beta).$$

Altogether we arrive at

$$z > C_0 \frac{e^{C_1 a^\beta}}{a^5},$$

where $C_0 = \frac{3}{4\pi\rho^3(1-2\rho)^2}e^{8K_0}$ and $C_1 = 2K_1(\chi_1^\beta + 3\chi_2^\beta)$. Optimizing over a we obtain minimum for $a = (\frac{5}{\beta C_1})^{\frac{1}{\beta}}$, i. e.,

$$z > C_0 e^{\frac{5}{\beta}} \left(\frac{\beta C_1}{5}\right)^{\frac{5}{\beta}}.$$

□

Proposition 4.8. There exists at least one Gibbs measure for the model $(\mathcal{LD}_4, \varphi_{HC})$ and every activity $z > 0$.

Proof.

(R) The range condition is proven in Lemma 4.6.

(S) Stability is satisfied because φ is non-negative, see Remark 4.3.

(Û) We choose M and Γ as in Subsubsection A.1.

(Û1) For all $\eta \in \mathcal{LD}_4(\mathbf{x})$ for $\mathbf{x} \in \Gamma^A$ such that $H_\Lambda(\mathbf{x}) < \infty$ we have $\chi(\eta) < \alpha$. This imposes a minimum density of points, since e. g. no ball with diameter α can be empty.

(Û2) We have number of summands $n_T \leq 32$, cf. Remark A.2, and thus the only quantity in question is φ_{HC}. By Remark A.3 we have $\chi(\eta) \leq a\chi_2(\rho)$, thus we only need to choose a and ρ such that $\chi_2(\rho) \leq \alpha/a$.

(Û3) $\Pi_\Lambda^z(\Gamma) > 0$ by Remark 4.4.

□

Using the same approach and the same pseudo-periodic configurations $\bar{\Gamma}$, it is straightforward to prove the existence of many different forms of unary hyperedge potentials. In the following, we suggest some alternate hyperedge potentials.

Remark 4.9. (Other smooth interaction potentials)
Alternate smooth interaction models could be considered using characteristics of k-faces of η instead of the circumdiameter. An example is the volume potential φ_V defined as a unary potential such that for $\eta \in \mathcal{L}D_4(\mathbf{x}), \mathbf{x} \in \bar{\Gamma}$ we have

$$\varphi_V(\eta, \mathbf{x}) \leq K_0 + K_1 \mathrm{V}(\eta)^\beta$$

for some $K_0, K_1 \geq 0, \beta > 0$, where $\mathrm{V}(\eta) = |\mathrm{conv}(\eta)|$ is the volume of the tetrahedron $\mathrm{conv}(\eta)$. Volume of a 3−simplex with positions $\eta' = \{x_0, x_1, x_2, x_3\} \subset \mathbb{R}^3$ can be calculated using the Cayley-Menger determinant [14], but the following expression [15] lends itself better to finding a bound:

$$V(\eta) = \left|\frac{1}{3!}\det(x_1 - x_0, x_2 - x_0, x_3 - x_0)\right|,$$

where the determinant of a 3×3 matrix with column vectors $x_1 - x_0, x_2 - x_0, x_3 - x_0$ can be bounded using Hadamard's inequality [6],

$$\det(x_1 - x_0, x_2 - x_0, x_3 - x_0) \leq \prod_{i=1}^{3} \|x_i - x_0\|.$$

Notice that we only need the length of three edges of the tetrahedron and that $\|x_i - x_0\| \leq a + 2\rho a$. Thanks to this, the potential value of both tetrahedra of type T_1 and T_2 can be bounded by

$$\varphi_V(\eta, \mathbf{x}) \leq K_0 + K_1 \left(\tfrac{1}{6}(a(1+2\rho))^3\right)^{\beta}, \quad \eta \in \mathcal{LD}_4(\mathbf{x}), \mathbf{x} \in \bar{\Gamma}.$$

The bound for the intensity z in the model $(\mathcal{LD}_4, \varphi_V)$ then becomes

$$z > \frac{3}{4\pi} e^{8K_0} \left(\frac{24K_1\beta e}{5}\right)^{\frac{5}{3\beta}} \frac{(\frac{1}{6}(1+2\rho)^3)^{\frac{5}{3}}}{\rho^3(1-2\rho)^2}. \tag{13}$$

Note that the same approach could be used for e. g. surface area of the tetrahedron, where we would simply replace $\frac{1}{6}(1+2\rho)^3$ by $\frac{4}{2}(1+2\rho)^2$ in (13).

Remark 4.10. (Other hardcore interaction potentials)
Other forms of the hard-core potential can be obtained relatively easily. For example, additional constraints can be added, e. g. minimum edge length $\ell > 0$. Finite horizons remain the same for all unary potentials, and therefore **(R)** holds. Stability **(S)** is satisfied, as the potential is still non-negative. The alternate upper regularity conditions **(Û1)** and **(Û3)** are satisfied for the same reasons. Care has to be taken for **(Û2)** to hold, since the pseudo-periodic configurations $\mathbf{x} \in \bar{\Gamma}$ now must satisfy the new criterion. This can be done by choosing a and ρ such that $a(1-2\rho) < \ell$.

Note also that while we have used the set $\mathcal{LD}_4$ for the definition of our models, it would be just as possible to consider the sets $\mathcal{LD}_2, \mathcal{LD}_3$, or even combinations of them.

Remark 4.11. (Optimality of the bounds)
Note that the bounds (12) and (13) are not optimal. Both are highly sensitive to the value of K_0, forcing it to be zero in practice, and especially for the model $(\mathcal{LD}, \varphi_S)$. For $\beta \leq 1$, the models are also sensitive to the value of K_1, but increasing β quickly weakens this dependence. The concrete values are easily very large, especially for the model $(\mathcal{LD}_4, \varphi_S)$, as the following table shows.

Model	K_0	K_1	β	Bound for z
$(\mathcal{LD}_4, \varphi_S)$	0	0.5	1	228,474
$(\mathcal{LD}_4, \varphi_S)$	0	1	10	36,908
$(\mathcal{LD}_4, \varphi_V)$	0	0.5	1	508
$(\mathcal{LD}_4, \varphi_V)$	0	1	2	338

A number of steps could be taken to improve the bound. For example, not all tetrahedra in any given tetrahedrization will attain the bounds χ_1 and χ_2. Furthermore,

(15) is unnecessarily conservative — see Remark (A.1). Finally, one may also be able to use an entirely different approach than that of [3] to obtain lower bounds.

Note that while the magnitude of the bounds might seem as a limitation, in practice one can always introduce a hard-core parameter which will not limit the model, but ensure that it exists for all $z > 0$. These bounds therefore have a theoretical, rather than practical value.

4.4. Laguerre models

4.4.1. Laguerre cell face interaction

In 3D we examine the Laguerre tessellation where every face contributes to the energy function. Since the potential depends on pairs of neighbouring cells having a common face, we talk about pair interaction.

Proposition 4.12. There exists at least one Gibbs measure for the hypergraph structure $\mathcal{LD}_2$, hyperedge potential $\varphi_{2,NVR}$ and every activity $z > 0$.

Proof.

(R) Remark 2.1 tells us that $\Delta = B(p'_\xi, \sqrt{p''_\xi + W})$ is the finite horizon for $(\xi, \mathbf{x}) \in \mathcal{LD}$ and unary hyperedge potential. Moreover it shows that the horizon can be decomposed to the ball with no interior points and annulus with width bounded by $\sqrt{W}$. Since the pair potential depends on two cells of $\eta = \{x_1, x_2\} \subset \mathbf{x}$. We define so-called Laguerre doubleflower, see Figure 1, $LF_2 := \bigcup_{\xi \in \mathcal{LD}_4, \xi \cap \eta \neq \emptyset} \bar{B}(p'_\xi, \sqrt{p''_\xi + W})$. For $y_1, y_2 \in LF_2$ one can find $\xi_1, \xi_2 \in \mathcal{LD}_4$ such that $y_1 \in \bar{B}(p'_{\xi_1}, \sqrt{p''_{\xi_1} + W})$ and $y_2 \in \bar{B}(p'_{\xi_2}, \sqrt{p''_{\xi_2} + W})$. Then either $\bar{B}(p'_{\xi_1}, \sqrt{p''_{\xi_1} + W}) \cap \bar{B}(p'_{\xi_2}, \sqrt{p''_{\xi_2} + W}) \neq \emptyset$ or $\bar{B}(p'_{\xi_1}, \sqrt{p''_{\xi_1} + W}) \cup \bar{B}(p'_\zeta, \sqrt{p''_\zeta + W}) \cup \bar{B}(p'_{\xi_2}, \sqrt{p''_{\xi_2} + W})$, $\eta \subset \zeta \in \mathcal{LD}_4$, is connected. Therefore the range condition holds with $l_R = 7$, $n_r = 0$, $\delta_R = 2\sqrt{W}$ and Laguerre doubleflower as the horizon for every $(\eta, \mathbf{x}) \in \mathcal{LD}_2$ and the hyperedge potential $\varphi_{2,NVR}$.

(S) Stability is satisfied because φ is non-negative, cf Remark 4.3.

(U) We choose M and Γ as in Subsubsection A.1.

(U1) By Remark A.4 there is $R_0 > 0$ such that $p''_\eta \leq R_0$ for all $\eta \in \mathcal{LD}_4(\mathbf{x}), \mathbf{x} \in \bar{\Gamma}^A$. For every $(\eta, \mathbf{x}) \in \mathcal{LD}$ the diameter of the set $\Delta = B(p'_\eta, \sqrt{p''_\eta + W})$, cf. Remark 2.1, can be bounded: $\operatorname{diam} \Delta = 2\sqrt{p''_\eta + W} \leq 2\sqrt{R_0 + W}$. In the case of Laguerre doubleflower LF_2 we obtain the bound for its radius $3\sqrt{R_0 + W}$. Since LF_2 is the horizon for every $(\eta, \mathbf{x}) \in \mathcal{LD}_2$ and the hyperedge potential $\varphi_{2,NVR}$, by Lemma 4.5 we have $r_\Gamma \leq 6\sqrt{R_0 + W}$.

(U2) $c_A^+ = sup_{\mathbf{x} \in \bar{\Gamma}^A} \sum_{\eta \in \mathcal{LD}_2(\mathbf{x}), \eta' \cap C \neq \emptyset} \frac{\varphi^+_{2,VNR}(\eta, \mathbf{x})}{card(\eta)} \leq \sum_{\eta \in \mathcal{LD}_2(\mathbf{x}), \eta' \cap C \neq \emptyset} \frac{K}{2}$, where the right side is finite since the sum is finite. Indeed the number of incident tetrahedra to each vertex is at most 32, cf. Remark A.2. Each incident tetrahedron contains

3 edges ending in the considered vertex. Therefore the number of summands is for sure ≤ 96.

(U3) The lower bound on z is gained from the condition $z|A| > e^{C_\Gamma}$, cf. Remark 4.4. Since $|A| = \frac{1}{3}\pi a^5 \rho^3 (1-2\rho)^2$ the inequality results in $z > C_0 \frac{1}{a^5} e^{C_1}$, where $C_0, C_1 > 0$ are constants not depending on a. Minimizing the right side over $a > 0$ we obtain $z > 0$ as $a \to \infty$.

□

4.4.2. Laguerre cell distribution interaction

The goal of the potential $\varphi^s_{k,T}$ is to influence the distribution of a geometric characteristic s computed from the sample of size k, $k \in \mathbb{N}$. In the stationary case the distribution on $\mathbf{x}$ is well approximated by the distribution on a finite η possessing a sample of size k large enough. For the simplicity of notation we have restricted ourselves to characteristics of single cells (3-facets) only. The next proposition (Proposition 4.13) is formulated and proved in this context. It can be straightforwardly extended to $0, 1, 2$-facets. The necessary technicalities concerning the hyperedge potential and the hypergraph structure were described in Remark 3.2.

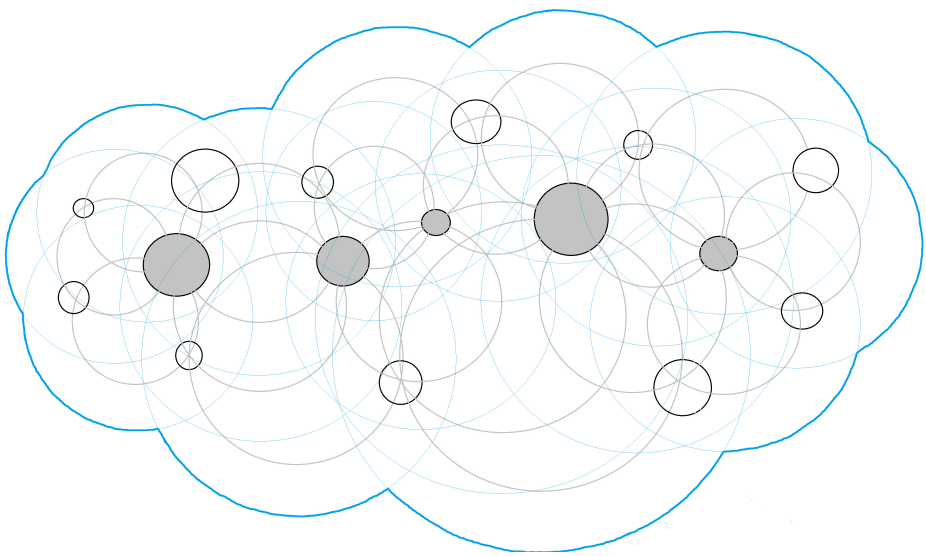

Fig. 1. Laguerre 5-flower LF_5 of grey generators. Black spheres depicture generators. Grey and blue spheres are their characteristic points and finite horizons, respectively.

Proposition 4.13. There exists at least one Gibbs measure for the hypergraph structure $\mathcal{CG}_{k,b}$, hyperedge potential $\varphi^s_{k,T}$, $k \in \mathbb{N}$, and every activity $z > 0$.

Proof.

(R) Remark 2.1 tells us that $\Delta = B(p'_\xi, \sqrt{p''_\xi + W})$ is the finite horizon for $(\xi, \mathbf{x}) \in \mathcal{LD}$ and unary hyperedge potential. Moreover it shows that the horizon can be decomposed to the ball with no interior points and annulus with width bounded by $\sqrt{W}$. The hyperedge η contains k points. Similarly as in Proposition 4.12 we define Lagurre k-flower, see Figure 1, $LF_k := \bigcup_{\xi \in \mathcal{LD}_4, \xi \cap \eta \neq \emptyset} \bar{B}(p'_\xi, \sqrt{p''_\xi + W})$. Then for $y_1, y_2 \in LF_k$ one can find $\xi_1, \xi_2 \in \mathcal{LD}_4$ such that $y_1 \in \bar{B}(p'_{\xi_1}, \sqrt{p''_{\xi_1} + W})$ and $y_2 \in \bar{B}(p'_{\xi_2}, \sqrt{p''_{\xi_2} + W})$. These two balls can be conected in the worst case by $k-1$ balls of the shape $\bar{B}(p'_\xi, \sqrt{p''_\xi + W})$, where $\mathrm{card}(\xi \cap \eta) \geq 2$. The range condition **(R)** is then satisfied with $l_R = 2k + 3$, $n_r = 0$, $\delta_R = 2\sqrt{W}$ and Laguerre k-flower as the horizon for every $(\eta, \mathbf{x}) \in \mathcal{CG}_{k,b}$ and the hyperedge potential $\varphi^s_{k,T}$.

(S) Stability is satisfied since φ is non-negative, cf Remark 4.3.

(U) We choose M and Γ as in Subsubsection A.1.

(U1) Since the radius of the set Δ of any $(\eta, \mathbf{x})$, $\eta \in \mathcal{LD}_4$, $\mathbf{x} \in \bar{\Gamma}^A$, can be bounded uniformly by $\sqrt{R_0 + W}$ the radius of the Laguerre k-flower LF_k is bounded by $(k+1)\sqrt{R_0 + W}$. Further by Lemma 4.5 the bound for r_Γ can be taken as $2(k+1)\sqrt{R_0 + W}$.

(U2) $c^+_A = sup_{\mathbf{x} \in \bar{\Gamma}^A} \sum_{\eta \in \mathcal{CG}_{k,b}(\mathbf{x}), \eta' \cap C \neq \emptyset} \frac{\varphi^s_{k,T}(\eta, \mathbf{x})}{card(\eta)} \leq \sum_{\eta \in \mathcal{CG}_{k,b}(\mathbf{x}), \eta' \cap C \neq \emptyset} \frac{K}{k}$, where the right side is finite since the sum is finite. Indeed the number of incident edges (vertices) to each vertex is at most 96, cf. proof of the previous Proposition 4.12. To each of these at most 96 vertices we can take again all his incident vertices. Repeating this $k-2$ times we obtain k-neighbourhood which is finite and we have finitely many possibilities how to choose k-tuple of vertices from it.

(U3) The lower bound on z is gained from the condition $z|A| > e^{c_\Gamma}$, cf. Remark 4.4. Since $|A| = \frac{1}{3}\pi a^5 \rho^3 (1-2\rho)^2$ the inequality results in $z > C_0 \frac{1}{a^5} e^{C_1}$, where $C_0, C_1 > 0$ are constants not depending on a. Minimizing the right side over $a > 0$ we obtain $z > 0$ as $a \to \infty$.

□

Corollary 4.14. The statement of the Proposition 4.13 holds for $T = dsc(H, H')$ and $K = \infty$.

Proof. Note that in the case of $T = dsc(H, H')$, it holds that $\varphi^s_{k,T} \leq K \wedge 2$. □

Remark 4.15. (On sublinearity in Delaunay tessellation)
Note that, in 2D we have the sublinearity of the cardinalities of the Delaunay edges and triangles thanks to the Euler's formula. This allows the parametrization of hyperedge potentials in Propositions 4.12 and 4.13 by a negative parameter. Unfortunately, the similar statement in the higher dimensions is not so obvious and no result about its validity is known.

5. SIMULATION

In [13] we presented an algorithm for the simulations of Gibbs–Laguerre tessellations in 3D. We were motivated by [4], where Gibbs Voronoi and Gibbs Delaunay tessellations in 2D were investigated. In the present paper we extend our models to Gibbs Delaunay–Laguerre tessellations.

5.1. Simulation of Gibbs tessellations on a finite window

In the present paper, stationary Gibbs Delaunay–Laguerre tessellations are investigated on $\mathbb{R}^3$. For simulations, it is necessary to approximate them inside a fixed observation window Λ. In our case the simulations are performed on the unit observation window in 3D, i. e., $\Lambda = [0,1]^3$. The finite volume Gibbs point process on Λ is such an approximation, see [10]. It is a probability measure absolutely continuous with respect to π_Λ. Its density f_Λ is given by (6), with Λ fixed. The outside configuration has to be specified. It cannot be empty since the resulting unbounded cells are undesirable. For that reason, the boundary effects are solved by periodic configuration. For $\mathbf{x} \in \Lambda = [0,1]^3$ the periodic configuration $\bar{\mathbf{x}}$ is obtained by an application of all integer shifts, i. e.,

$$\bar{\mathbf{x}} = \cup_{i \in \mathbb{Z}^3} \cup_{x \in \mathbf{x}} \tau_i(x),$$

where $\tau_i : \mathbb{R}^3 \mapsto \mathbb{R}^3$ is the shift by a vector $i \in \mathbb{Z}^3$.

Because of the complexity of Gibbs point processes and the unknown value of partition function Z_Λ, the Markov chain Monte Carlo (MCMC) techniques are used to carry out the simulations. The Metropolis-Hastings birth-death-move (MHBDM) algorithm enables the simulation of finite point processes with a density with respect to π_Λ. For a general version of the algorithm see [8]. The detailed algorithm for simulations of Gibbs–Laguerre tessellations is available in [13], including the proposal distributions used here. Several parameters have to be specified, in our case $W = 0.15$ (upper bound of the space of marks) and $z = 1000$ (activity).

The computations of the Laguerre tessellations are done by Voro++, an open-source software library [12]. Voro++ allows the recomputation of individual cells which is necessary for the local computations of the tessellations. In each step of the MHBDM algorithm the energy of the tessellation has to be evaluated. This is very time demanding if done for the whole tessellation. Since not all of the cells have been changed, it is sufficient to recompute only a necessary set of cells that have undergone a change. The algorithm for finding such cells is described in [11].

5.2. Simulation study

In order to give a vivid description of the model, we would like to simulate Gibbs–Laguerre tessellation whose energy consists of a single potential $\varphi^s_{k,T}$, defined in (9), multiplied by a real parameter θ. This type of hyperedge potential is important in practice as it allows simulation of tessellations that are similar to real data in terms of the distribution of a chosen geometric characteristic, see [13].

Here, the sphericity is considered as the cell characteristic s. It is defined by the formula

$$s = \frac{\pi^{1/3}(6 \cdot \text{volume})^{2/3}}{\text{surface area}}.$$

The functional T is the histogram discrepancy, i. e., $T(s(\cdot)) = \text{dsc}(H_{s(\cdot)}, H'_s)$. The constant s_0 is set to be 0. The histogram of sphericity H'_s, given by a real data, is plotted in Figure 2. In case of $\theta > 0$, the existence of this model in $\mathbb{R}^3$ is ensured by Corollary 4.14 for an arbitrary activity $z > 0$.

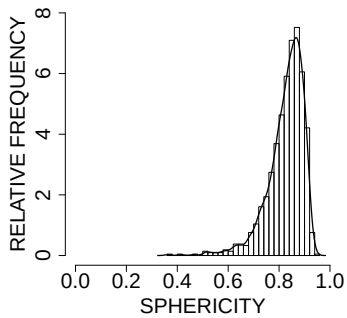

Fig. 2. Prescribed sphericity distribution for the simulations of Gibbs Laguerre tessellation.

The problem with the potential (9) is that the computational time increases rapidly with increasing k and a large k is necessary for a good approximation of the overall distribution on the entire $\mathbf{x}$. In order to evaluate the change of the energy (caused by addition/deletion or movement of a generator) in each iteration of the MHBDM algorithm, all connected k-tuples of cells where at least one cell was changed have to be considered. The number of such k-tuples is enormous for a large k causing the computational time to become excessively long. To handle this problem, we modify the potential $\varphi^s_{k,T}$, (9), for the purposes of simulations in a bounded window. Instead of the fixed number k of cells per hyperedge, we evaluate the potential over all cells with their generators inside the window, i. e.,

$$\varphi^s_{\Lambda,T}(\bar{\mathbf{x}}) = \left(|T(s(\{L_x : x \in \bar{\mathbf{x}},\ x \in \Lambda\})) - s_0|\right)^{1/2} \wedge K. \tag{14}$$

This modification leads to a significant improvement in computational time, since the distributional characteristics (sample mean, sample variance or histogram) of the entire

tessellation can be computed only once for the initial configuration. Then they are easily modified in each iteration since only a small number of cells differ in the proposal. The drawback is that the range condition **(R)** no longer holds in the case of (14) since $\varphi^s_{\Lambda,T}$ admits a variable number of cells in its argument. This fact is irrelevant for finite volume Gibbs processes.

θ	total number of cells	discrepancy
-10000	349	1.57805
-5000	374	1.578
-2000	468	1.441
-1500	805	1.076
-1000	846	0.9386
-1	950	0.573
1	1018	0.566
1000	1020	0.187
1500	985	0.0175
10000	1000	0.0169

Tab. 1. Dependency of numerical characterisctics on the value of the parameter θ.

The choice of the parameter θ determines the properties of the model. The presented simulation study shows the influence of θ on the sphericity distribution, the discrepancy, and the number of non-empty cells in Λ. Numerical results are summarized in Table 1 and Figures 3 and 5. Note that $\theta < 0$ violates the stability condition **(S)** since we are not able to ensure the sublinearity of $\mathcal{CG}_{k,b}$ in 3D, cf. Remark 4.15. On the other hand, even simulations of the model with $\theta < 0$ are interesting from a practical point of view.

With an increasing value of the parameter θ the discrepancy decreases, i. e., the sphericity distribution of simulated tessellations is getting closer to the prescribed one. As θ decreases, the tessellations become quite different. Instead of moving horizontally, corresponding to less spherical cells occurring, the peak of the density curve increases, i. e., sphericities in the narrow range are favoured. This causes a dramatic increase of discrepancy which suddenly stops below the value 1.58. This behaviour is observable for $\theta = -5000$ and smaller. Narrowness of the density means that all cells in the tessellation have very similar sphericity and are in this sense rigid. The densities for values $-1, 1$ are quite similar. For $\theta = 1500$, the density is quite similar to the prescribed one and any further increase of the parameter value has only a negligible effect on the decay of the discrepancy. The discrepancies fluctuate more for smaller (in absolute value) values of θ. The fluctuations are considerably smaller for values ≤ -5000 and ≥ 1500. The same phenomenon is observable for the number of cells. Moreover the number of cells rapidly decreases with decreasing negative values of θ. 3D visualizations of the simulated realizations for $\theta = -10000$ and $\theta = 1500$ are available in Figure 4 (note that the numbers of cells differ significantly).

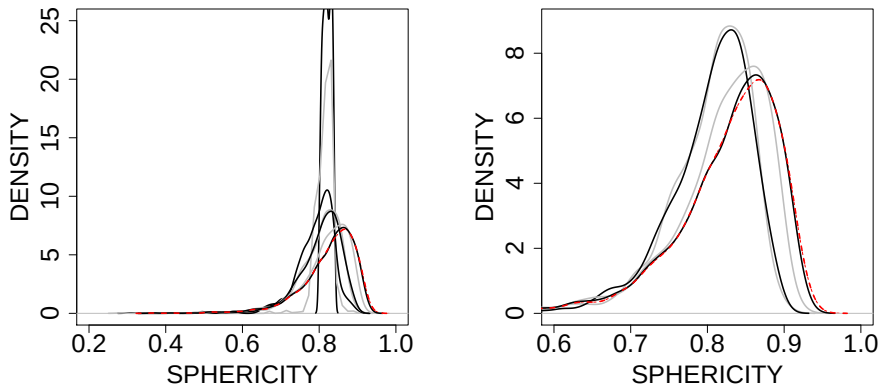

a) b)

Fig. 3. Densities of the sphericity distribution in MCMC simulations of Gibbs Laguerre tessellations. The dashed line represents the prescribed sphericity distribution, cf. Figure 2. Black and grey full lines are densities coming from simulations. In diagram a) densities for θ equal to $-10000, -2000, -1000, -1, 1, 1000, 1500$ have their peak magnitudes in the descending order. In diagram b) the detail of diagram a) is present for θ equal to $-1, 1, 1000, 1500$.

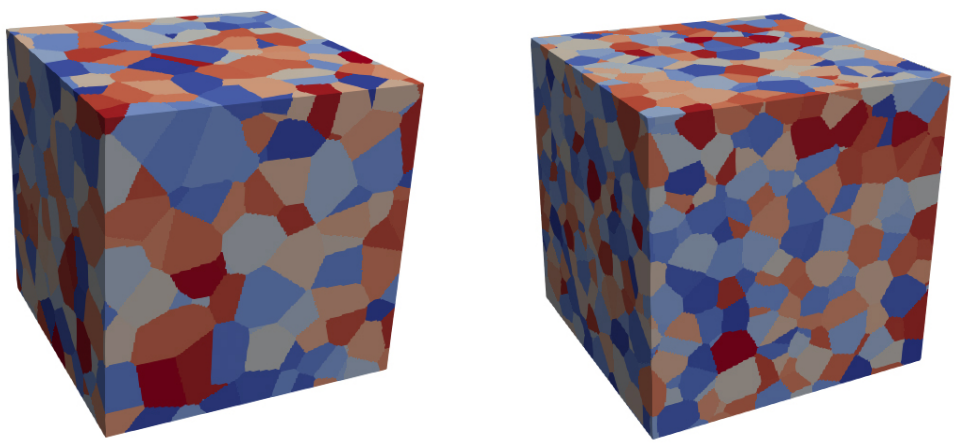

a) b)

Fig. 4. The 3D simulations of the sphericity model for $\theta = -10000$, a), and $\theta = 1500$, b). The colouring is random.

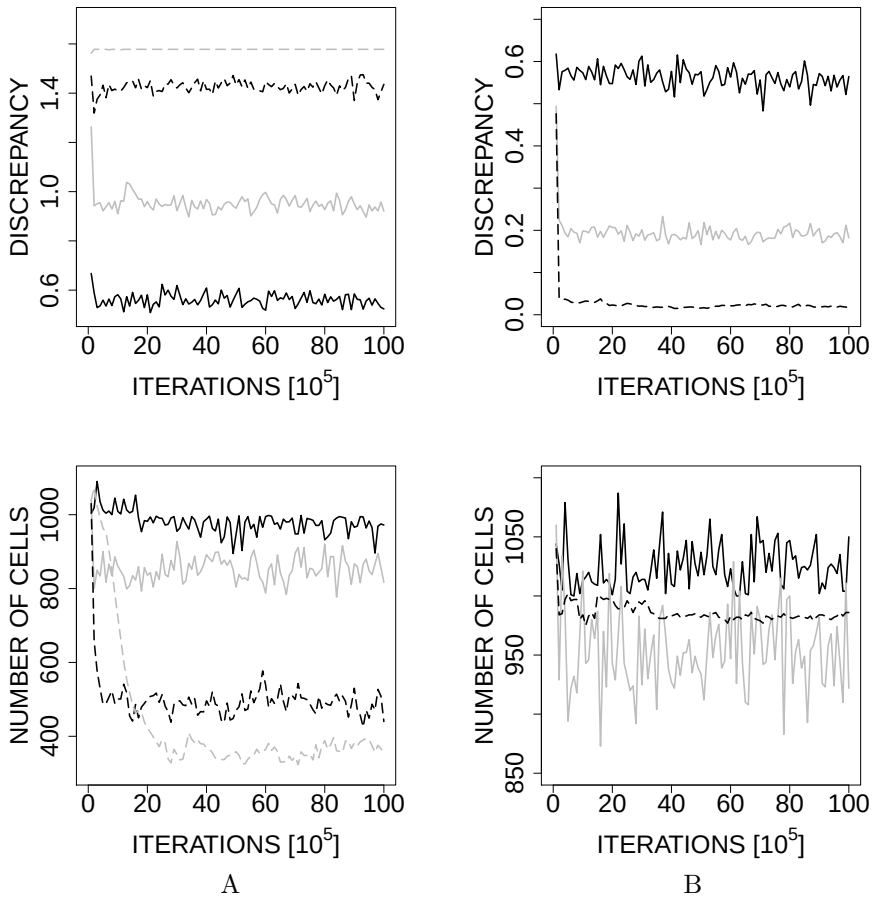

Fig. 5. Discrepancy between simulated and prescribed histogram (up) and number of cells (down) for varying values of the parameter θ in MCMC simulations of Gibbs Laguerre tessellations. In column A and B the negative and positive values of parameter θ are involved, respectively. Namely in column A, $\theta = -1$ corresponds to black full line, $\theta = -1000$ to grey full line, $\theta = -2000$ to black dashed line and $\theta = -10000$ to grey dashed line. In column B, $\theta = 1$ corresponds to black full line, $\theta = 1000$ to grey full line and $\theta = 1500$ to black dashed line. We draw each 10^5th iteration.

At the first sight, the interaction introduced by potentials (9) appears to be scale invariant. In that case, the intensity of the Gibbs point process could be changed by just changing the activity parameter z without changing the shape of cells. This was neither proved nor observed yet. Unfortunately, this property is for sure lost in the case

of the modification (14) since the distributional characteristics are sensitive to the size of the sample from which they are evaluated and the potential (14) works with samples of various sizes. Finally, let us note that the intensity of Gibbs point process is not in general the same as the intensity of Laguerre cells (non-empty from definition). These two intensities can equal if a hardcore condition forbidding empty cells is introduced. Then the scale invariance is lost again.

APPENDIX

A. PSEUDO-PERIODIC CONFIGURATIONS

When dealing with the existence problem of Gibbs models, we can restrict ourselves to so-called pseudo-periodic configurations, a key concept in the verification of the upper regularity condition **(U)**, see Subsection 4.1 and [3].

Let $M \in \mathbb{R}^{3\times 3}$ be an invertible 3×3 matrix with column vectors (M_1, M_2, M_3). For each $k \in \mathbb{Z}^3$ define the cell

$$C(k) = \{Mx \in \mathbb{R}^3 : x - k \in [-1/2, 1/2)^3\}.$$

These cells partition $\mathbb{R}^3$ into parallelepipeds, i. e., solids whose six faces are all parallelograms in $\mathbb{R}^2$. We write $C = C(0)$. Let $\Gamma \subset \mathbf{N}_C$ be measurable and non-empty. Then we define the pseudo-periodic configurations $\bar{\Gamma}$ as

$$\bar{\Gamma} = \{\mathbf{x} \in \mathbf{N} : \vartheta_{Mk}\mathbf{x}_{C(k)} \in \Gamma \text{ for all } k \in \mathbb{Z}^3\},$$

the set of all configurations whose restriction to $C(k)$, when shifted back to C, belongs to Γ. The prefix pseudo- refers to the fact that the configuration itself does not need to be identical in all $C(k)$, it merely needs to belong to the same class of configurations.

A.1. Configuration for $\mathbb{R}^3$ tetrahedrization

Here we introduce and analyze the pseudo-periodic configuration used in the proofs of existence of our tessellation models. Fix some $A \subset C \times S$ and define

$$\Gamma^A = \{\zeta \in \mathbf{N}_C : \zeta = \{p\}, p \in A\},$$

the set of configurations consisting of exactly one point in the set A. The set of pseudo-periodic configurations $\bar{\Gamma}$ thus contains only one point in each $C(k), k \in \mathbb{Z}^3$.

Let M be such that $|M_i| = a > 0$ for $i = 1, 2, 3$ and $\angle(M_i, M_j) = \pi/3$ for $i \neq j$. We choose

$$A = B(0, \rho a) \times \left[0, \left(\frac{a}{2}(1 - 2\rho)\right)^2\right] \tag{15}$$

in order for balls to never overlap. Hence no problems with point redundancy occur. We choose $\rho < 1/4$ in order for points to remain in a general position.

Remark A.1. (Nonredundancy of points)
The interval for radii in (15) is too conservative since we can admit balls to partially overlap and instead of $\left(\frac{a}{2}(1 - 2\rho)\right)^2$ use $(a(1 - 2\rho))^2$ as an upper bound. Then the balls may overlap but not over its centers. Therefore the nonredundancy of points is still preserved.

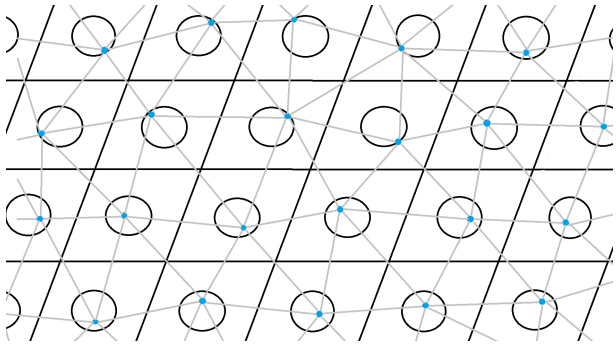

Fig. 6. An example of pseudo-periodic configuration for unmarked points in 2D.

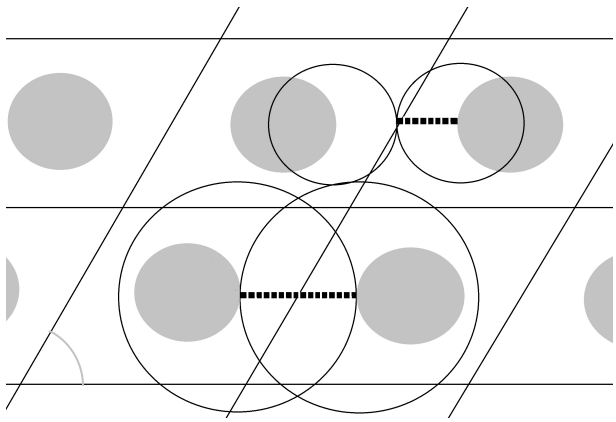

Fig. 7. Nonredundancy of points in 2D. Spatial parts of sets A, i. e., $B(0, \rho a)$, are gray. Black circles are marked points with the maximal radii represented by bold interrupted line of the length $\frac{a}{2}(1-2\rho)$ and $a(1-2\rho)$ in the upper and lower part of the picture, respectively. Those in the upper part do not overlap and those in the lower part do not overlap over center.

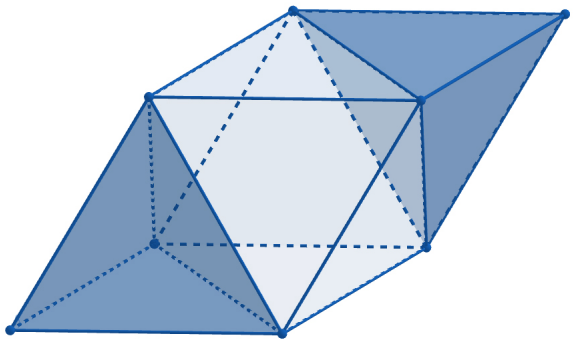

Fig. 8. Tetrahedral-octahedral honeycomb.

A useful mental model of how to think of the class $\bar{\Gamma}$ is to start from a configuration

$$\mathbf{x}_0 = \{(M_a k, 0) \in \mathbb{R}^3 \times S : k \in \mathbb{Z}^3\} \in \bar{\Gamma},$$

with points at the centers of the set A and then imagine any configuration $\mathbf{x} \in \bar{\Gamma}$ as a perturbed version of $\mathbf{x}_0$. In the following remark we describe how the tetrahedrizations formed by $\mathbf{x}_0$ look like. The tetrahedrization of any $\mathbf{x} \in \bar{\Gamma}$ is considered as a perturbed version of tetrahedrization of $\mathbf{x}_0$. When speaking about these perturbed tetrahedrizations we will shortly say: "up to a perturbation".

Remark A.2. (Pseudo-periodic tessellation)
While in the two-dimensional case [3] the point configuration forms a tessellation out of equilateral triangles (up to a perturbation), the three-dimensional case results into the so-called tetrahedral-octahedral honeycomb (up to a perturbation), cf. Figure 8. This tessellation, if tetrahedrized, contains two different types of tetrahedra : a regular tetrahedron with side length a and an irregular tetrahedron with side lengths $(a, a, a, a, a, \sqrt{2}a)$, again, up to a perturbation. We will refer to a tetrahedron that is a perturbed version for the regular tetrahedron as T_1 and similarly T_2 for the irregular tetrahedron. In the tetrahedron-octahedron tessellation, each vertex is incident to eight regular tetrahedra and six regular octahedra, cf. Figure 9. Since each octahedron contains four tetrahedra, we obtain the bound for n_T, the number of incident tetrahedra of each vertex, $n_T \leq 8 + 6 \cdot 4 = 32$.

To show that the range of interactions is limited for the configurations in $\bar{\Gamma}$ two quantities need to be shown to be uniformly bounded. The first one is the circumdiameter of the tetrahedra described in Remark A.2.

Remark A.3. (Bounding the circumdiameter of tetrahedra)
As noted in Remark A.2, there are two types of tetrahedra in the tetrahedrization, T_1 and T_2. The following argument describes how to obtain the bound for the regular tetrahedron (T_1), but the same procedure applies to T_2 as well. The optimization problem

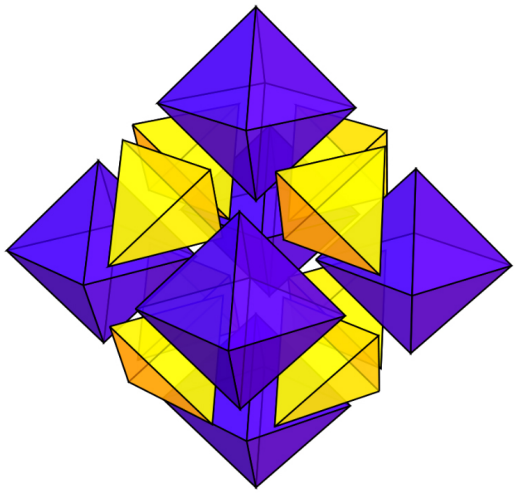

Fig. 9. [5] Tetrahedral-octahedral honeycomb tessellate in 3D. Each vertex is incident to eight regular tetrahedra (yellow) and six regular octahedra (blue), which are shown in an exploded view.

to be solved is

$$\begin{aligned} &\underset{x_1,x_2,x_3,x_4\in\mathbb{R}^3}{\text{maximize}} && \chi(\{x_1,x_2,x_3,x_4\}) \\ &\text{subject to} && \|x_i - t_i\| \le \rho a, \quad t_i \in \mathbb{R}^3, i = 1,2,3,4, \\ &&& \|t_i - t_j\| = a, \quad i = 1,2,3,4. \end{aligned} \tag{16}$$

An essential finding is that the points $x_1, \ldots, x_4$ which maximize the circumdiameter χ form a sphere tangent[1] to the spheres $\mathbb{S}_i := \partial B(t_i, \rho a), i = 1, \ldots, 4$. This reduces the number of possible solutions to 2^4 (even less because of symmetry) and all that remains is to check the largest solution. If $t_i = (t_{i,1}, t_{i,2}, t_{i,3})$, $i = 1,2,3,4$, then we are looking for a sphere $\mathbb{S} = \partial B(y, r)$, $y = (y_1, y_2, y_3) \in \mathbb{R}^3$, such that

$$(y_1 - t_{i,1})^2 + (y_2 - t_{i,2})^2 + (y_3 - t_{i,3})^2 = (r - e_i \rho a)^2, \quad i = 1,2,3,4,$$

where $e_i = \pm 1$, creating the said 2^4 possible solutions. It is possible to linearize these equations. Solving linear equations and choosing the solution yielding the largest circumradius give the following bounds. For $T1$ tetrahedra, we obtained the bound

$$\chi_1(\rho) := 2(\sqrt{6}/4 + \rho)$$

and the maximum in (16) is $a\chi_1(\rho)$. For T2, we obtain the bound

$$\chi_2(\rho) := 2\frac{2\rho + \sqrt{2 - 32\rho^2 + 64\rho^4}}{2 - 32\rho^2},$$

[1] Spheres are said to be tangent if they intersect at a point.

and the maximum is $a\chi_2(\rho)$. Both cases are valid for $\rho < 1/4$.

The second quantity to be bounded is the weight of a characteristic point.

Remark A.4. (Bounding the weight of the characteristic point)
Since the perturbation happens on a bounded window and the points' weights are bounded, this amounts to proving that the points cannot come arbitrarily close to, or even attain, a coplanar position. However, this is equivalent to the boundedness of the circumdiameter of the tetrahedron, which we have already proven.

ACKNOWLEDGEMENT

The research of Filip Seitl was supported by Charles University, project GAUK 154119. The research of Daniel Jahn work was supported by Czech Science Foundation, project 17-00393J. We thank to prof. Viktor Beneš for helpful comments and suggestions.

(Received August 27, 2019)

REFERENCES

[1] S. N. Chiu, D. Stoyan, W. S. Kendall, and J. Mecke: Stochastic Geometry and its Applications. J. Willey and Sons, Chichester 2013. DOI:10.1002/9781118658222

[2] D. Dereudre: Introduction to the theory of Gibbs point processes. In: Chapter in Stochastic Geometry, pp. 181–229, Springer, Cham 2019. DOI:10.1007/978-3-030-13547-8_5

[3] D. Dereudre, R. Drouilhet, and H. O. Georgii: Existence of Gibbsian point processes with geometry-dependent interactions. Probab. Theory Rel. *153* (2012), 3, 643–670. DOI:10.1007/s00440-011-0356-5

[4] D. Dereudre and F. Lavancier: Practical simulation and estimation for Gibbs Delaunay–Voronoi tessellations with geometric hardcore interaction. Comput. Stat. Data An. *55* (2011), 1, 498–519. DOI:10.1016/j.csda.2010.05.018

[5] Fropuff: The vertex configuration of a tetrahedral-octahedral honeycomb. (2006), `https://en.wikipedia.org/wiki/File:TetraOctaHoneycomb-VertexConfig.svg`

[6] P. Hadamard: Résolution d'une question relative aux déterminants. Bull. Sci. Math. *17* (1893), 3, 240–246.

[7] C. Lautensack and S. Zuyev: Random Laguerre tessellations. Adv. Appl. Probab. *40* (2008), 3, 630–650. DOI:10.1017/s000186780000272x

[8] J. Møller and R. P. Waagepetersen: Statistical Inference and Simulation for Spatial Point Processes. Chapman and Hall/CRC, Boca Raton 2003. DOI:10.1201/9780203496930

[9] A. Okabe, B. Boots, K. Sugihara, and S.N. Chiu: Spatial Tessellations: Concepts and Applications of Voronoi Diagrams. J. Willey and Sons, Chichester 2009. DOI:10.2307/2687299

[10] C. Preston: Random Fields. Springer, Berlin 1976. DOI:10.1007/bfb0080563

[11] R. Quey and L. Renversade: Optimal polyhedral description of 3D polycrystals: Method and application to statistical and synchrotron X-ray diffraction data. Comput. Method Appl. M *330* (2018), 308–333. DOI:10.1016/j.cma.2017.10.029

[12] C. Rycroft: Voro++: A three-dimensional Voronoi cell library in C++. Chaos *19* (2009), 041111. DOI:10.1063/1.3215722

[13] F. Seitl, L. Petrich, J. Staněk, C. E. Krill III, V. Schmidt, and V. Beneš: Exploration of Gibbs-Laguerre Tessellations for Three-Dimensional Stochastic Modeling. Methodol. Comput. Appl. Probab. (2020). DOI:10.1007/s11009-019-09757-x

[14] D. M. Y. Sommerville: An Introduction to the Geometry of N Dimensions. Methuen and Co, London 1929.

[15] P. Stein: A note on the volume of a simplex. Amer. Math. Monthly *73* (1966), 3, 299–301. DOI:10.2307/2315353

[16] H. Zessin: Point processes in general position. J. Contemp. Math. Anal. *43* (2008), 1, 59–65. DOI:10.3103/s11957-008-1005-x

Daniel Jahn, Department of Probability and Mathematical Statistics, Charles University, Sokolovská 83, 186 75 Praha 8. Czech Republic.
e-mail: jahn@karlin.mff.cuni.cz

Filip Seitl, Department of Probability and Mathematical Statistics, Charles University, Sokolovská 83, 186 75 Praha 8. Czech Republic.
e-mail: seitl@karlin.mff.cuni.cz